

D. MIKUSEK¹, C. RAPIEJKO^{1*}, A. ANDRZEJCZAK¹, T. PACYNIAK¹**BENEFIT EFFECT OF LOW ADDITION YTTRIUM ON THE PHASE α_{Mg} AND EUTECTIC $\alpha_{Mg} + \gamma(Mg_{17}Al_{12})$ IN AZ91 ALLOY**

This paper presents results of a study of the effect of inoculation of yttrium on the microstructure of AZ91 alloy. The concentration of the inoculant was increased in samples in the range from 0.1% up to 0.6%. The influence of Y on the thermal effects resulting from the phase transformations occurring during the crystallisation at different inoculant concentrations were examined with the use of Derivative and Thermal Analysis (DTA). The microstructures of the samples were examined with the use of an optical microscope; and an image analysis with a statistical analysis were also carried out. Those analyses aimed at examining the effect of inoculation of the Y on the differences between the grain diameters of phase α_{Mg} and eutectic $\alpha_{Mg} + \gamma(Mg_{17}Al_{12})$ in the prepared examined material as well as the average size of each type of grain by way of measuring their perimeters.

Keywords: magnesium alloy AZ91, yttrium, grain refining, solidification process, investment casting

1. Introduction

The general trend, since 1920 when concept of strength-to-weight ratio has been proposed, in all maritime, air and ground transportation is the permanent research of new metal alloy that has a higher strength-to-weight ratio to reduce the cost of carrying [1-2]. Optimizing the chemical composition and microstructure of those alloys improves their rheological as well as physical and chemical properties and thus provides new fields of application potentials. Two aspects has to be taken into consideration; facility and cost manufacturing and its usage properties. As magnesium alloys known for its castability and low density (about 1.74 g/cm³) and are additionally facilities of machining, they find numerous applications in various industrial branches, e.g. aviation, motorization, etc. [3].

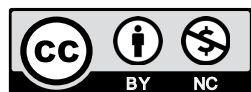
The biggest effect on the properties of a ready cast is exerted by the applied casting technology, the used materials and the subsequent thermal treatment [2,4,5]. The best properties of the casts are obtained by means of pressure casting [6]. Other methods of obtaining magnesium alloy casts include the use of ceramic, permanent and sand moulds, which do not provide casts with sufficiently good properties, due to too massive precipitation of the phases in the microstructure of the obtained casts [1,2,4]. One of the methods of improving the mechanical properties of the casts is intensive cooling of the moulds, which makes it possible

to obtain a relative good microstructure, which, in consequence, improves the properties [7]. A inoculation of the microstructure of a cast obtained in the as-cast state can be achieved also as a result of introducing inoculants or alloy additions [8-15].

The process of inoculation can be carried out with the use of different elements, including rare earth metals. An element belonging to the group of rare earths is yttrium, which is used as an alloy addition to magnesium alloys and which also plays the role of an inoculant [2]. Yttrium has a significant effect on the microstructure and properties of magnesium alloys. Ch. Jun et al., in their study [16], demonstrated that the application of yttrium in the concentration of 1.2% increases the tensile and elongation strength. In turn, the work [9] proves that an yttrium (Y) addition in the amount of 5% and 10% improves the compressive strength of magnesium alloys, and e.g. the magnesium alloy Mg-2.2Y has a higher tensile strength than the classical magnesium alloy AZ31 [16]. Also, an introduction of yttrium in the amount of 0.5% makes it possible to obtain the highest hardness as well as strength properties of all the examined alloys [18]. On the other hand, Zude Zhao et. al. in their research [19], disclosed that the 1.76% of yttrium addition improve yield strength, ultimate tensile strength and elongation. What is more, they demonstrated that alloy can be thixoformed which causes higher value of yield strength, ultimate tensile strength and elongation in comparison to standard method of melting.

¹ LODZ UNIVERSITY OF TECHNOLOGY, DEPARTMENT OF MATERIAL ENGINEERING'S AND PRODUCTION SYSTEMS, 1/15 STEFANOWSKIEGO STR., 90-924, LODZ, POLAND

* Corresponding author: cezary.rapiejko@p.lodz.pl



Nevertheless, Xianhua Chen et. al. [20] studied impact of yttrium on the microstructure, electromagnetic interference (EMI) shielding effectiveness (SE) and mechanical properties of Mg-Zn-Y-Zr alloys. They came up with conclusions that higher addition of yttrium gave decreased of grain size, but 1.90% of yttrium addition was optimal to achieve the higher EMI shielding capacity.

Recent literature focuses primarily on Y as alloying element. It influence on formation of new phases which improve the properties of the examined alloys. Therefor is no unequivocal information on the effect of yttrium small amounts on microstructure and mechanical properties of magnesium alloys, which influence is such as an inoculant (or modifying agent), not as alloying element.

The aim of the research was to examine the effect of the yttrium inoculation process the thermal effects resulting from the phase transformations occurring during the crystallization and on the grain fragmentation of the microstructure of examined AZ91 alloys obtained in ceramic moulds.

2. Experimental

The investigations included the preparation of 7 melts for alloy AZ91, which was subjected to inoculation with yttrium (Y). The melt schedule has been presented in Table 1. Exactly the same mass percentage of the inoculant was used in all the melts. Yttrium was introduced to melts in MgY master alloy which composition has been shown in Table 2.

TABLE 1

Melt schedule

Melt number	Melt's chemical composition
I	AZ91
II	AZ91 + 0.1% (mass) Y
III	AZ91 + 0.2% (mass) Y
IV	AZ91 + 0.3% (mass) Y
V	AZ91 + 0.4% (mass) Y
VI	AZ91 + 0.5% (mass) Y
VII	AZ91 + 0.6% (mass) Y

TABLE 2

Chemical composition of MgY master alloy

Chemical composition, % wt.					
Mg	Y	Fe	Ni	Al	Si
69.55	29.97	0.41	0.01	0.03	0.02

For the examinations, alloy AZ91 was selected, the composition of which has been shown in Table 3. The composition of the examined alloy is in accordance with the international standard PN-EN 1753:2001 [21].

Each time, the alloy was melted in a crucible, which was heated in a resistance furnace SNOL 8,2/1100 UMEGA AB to the temperature of $740^{\circ}\text{C} \pm 5^{\circ}\text{C}$. In order to prevent oxidation

TABLE 3

Chemical composition of alloy AZ91

Chemical composition, % wt.					
Mg	Al	Zn	Mn	Ca	Si
91.2	7.90	0.634	0.160	0.0013	0.0147

of the magnesium alloys, sulphur powder was applied. After the examined alloys were cast, they were cooled down at room temperature.

The casts were made in ceramic mould – TDA samplers preheated to 180°C . Inside the samplers, a quartz pipe, sealed on one side, served as a shield for a measuring thermocouple type S (Pt-PtRh10). The samplers were made according to the technology described in [22]. The investigations of the solidification and crystallization of the examined alloys were performed by means of the TDA method [23], according to the methodology developed by authors of this publication and described in [7] on the test bench presented in [22].

An evaluation of the cooling ($t = f(\tau)$), kinetics ($dt/d\tau = f'(\tau)$) and crystallization process was made by the TDA method. On the derivation curve ($dt/d\tau = f'(\tau)$), the following thermal effects for the examined magnesium alloys were marked with points:

$P_k - A - D$ – crystallization of primary phase α_{Mg} ,

$D - E - F - H$ – crystallization of eutectic $\alpha_{\text{Mg}} + \gamma(\text{Mg}_{17}\text{Al}_{12})$.

The chemical composition of the samples was tested with the use of a spark spectrometer SPECTROMAXx – Spectro. In order to reveal the microstructure of the ground and polished samples, the latter was subjected to etching. For the etching, a formulation containing 1 ml acetic acid, 50 ml distilled water and 150 ml ethyl alcohol was used. The microstructure test was performed with the use of an optical microscope Nikon Eclipse Ma 200, and the image analysis combined with a statistical analysis were carried out by means of a computer program working with a NIS-Elements microscope. The results of the TDA analysis and the statistical analysis for the inoculated samples were presented in reference to the initial alloy AZ91, not inoculated with yttrium.

3. Results and discussion

TDA test

Figure 1 shows exemplary TDA characteristics for alloy AZ91 + 0.1% (mass) Y, whereas Table 4 compiles the coordinates of the characteristic points and their values for alloy AZ91.

For the examined alloys, the TDA characteristics were recorded and the values for the particular characteristic points of the microstructure crystallization were determined. Based on the TDA data, the solidification times for primary phase α_{Mg} and eutectic $\alpha_{\text{Mg}} + \gamma(\text{Mg}_{17}\text{Al}_{12})$ were calculated. The calculations were made from the formula:

- Solidification time of phase α_{Mg} :

$$\Delta\tau_{\alpha} = \tau_D - \tau_{pk}$$

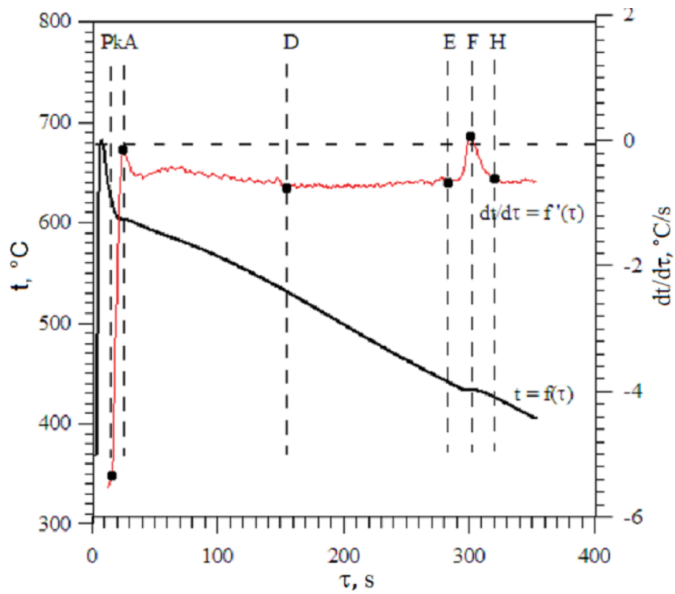


Fig. 1. TDA characteristics of alloy AZ91 + 0.1% (mass) Y solidifying in a ceramic sampler ATD10C-PL

- Solidification time of eutectic $\alpha_{Mg} + \gamma(Mg_{17}Al_{12})$:

$$\Delta\tau_{D\gamma} = \tau_H - \tau_D.$$

In order to present the effect of the inoculation on the TDA characteristics in reference to the non-inoculated alloy AZ91, the differences in the crystallization times of primary phase α_{Mg} and eutectic $\alpha_{Mg} + \gamma(Mg_{17}Al_{12})$ were calculated from the formula:

- Difference in the solidification time of phase α_{Mg} :

$$\Delta\tau_{D\alpha} = \Delta\tau_{\alpha AZ91} - \Delta\tau_{\alpha AZ91 in X},$$

- Difference in the solidification time of eutectic $\alpha_{Mg} + \gamma(Mg_{17}Al_{12})$:

$$\Delta\tau_{D\gamma} = \Delta\tau_{\gamma AZ91} - \tau_{\gamma AZ91 in X}.$$

where: *inX* denotes the amount of the introduced inoculant.

The calculation results have been given in Figure 2.

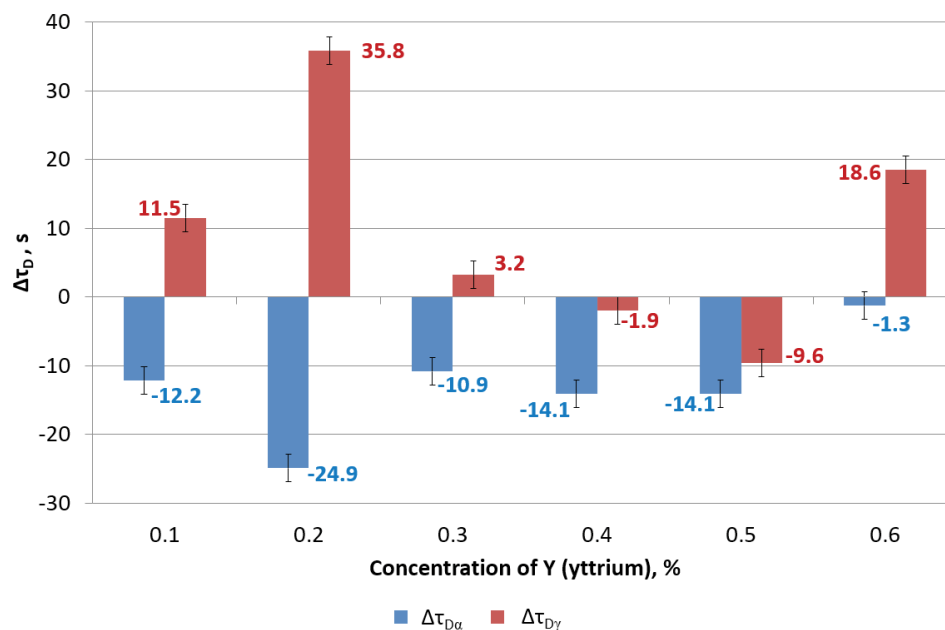


Fig. 2. Difference in the solidification time of phase α_{Mg} and eutectic $\alpha_{Mg} + \gamma(Mg_{17}Al_{12})$ of inoculated alloys Y in reference to the initial alloy AZ91

It can be inferred from the diagram shown in Figure 2 that introducing yttrium into alloy AZ91 changes the crystallization time of both the primary phase α_{Mg} and the eutectic phase $\alpha_{Mg} + \gamma(Mg_{17}Al_{12})$. The crystallization time of phase α_{Mg} , depending on the amount of the introduced inoculant, is reduced. The shortest crystallization time of the primary phase α_{Mg} was observed for the yttrium concentration of 0.2%, which equalled about 25 s. For the yttrium content of 0.6%, the crystallization time of the primary phase was shorter only by 1.3 s compared to the non-inoculated alloy AZ91. The crystallization time of the eutectic phase $\alpha_{Mg} + \gamma(Mg_{17}Al_{12})$ increased in the yttrium concentration range from 0.1% to 0.3%, reaching the highest increase equalling 35.8 s for 0.2% of the inoculant concentration. Applying the yttrium concentration in the range from 0.3% to 0.5% shortened the crystallization time of the eutectic phase. The biggest reduction of the crystallization time of phase $\alpha_{Mg} + \gamma(Mg_{17}Al_{12})$ equalling 14.1 s was observed for the inoculant concentration of 0.4% and 0.5%. In turn, the total crystallization time increases in the case of the inoculant concentrations of 0.2% and 0.6%. For the remaining inoculant concentrations, the crystallization time becomes shorter. The biggest reduction of the total crystallization time, which equalled 23.7 s, was observed for the concentration of 0.5%.

Microstructure analysis

In order to evaluate the degree of microstructure refinement, metallographic analyses were performed for the obtained alloys. Images of the microstructures were taken, which were then subjected to an image analysis, described in the further section of this study. Figure 3 shows an exemplary microstructure of a inoculated alloy AZ91 + 0.5%Y. It can be inferred from the performed metallographic tests that, in the AZ91 alloy in-

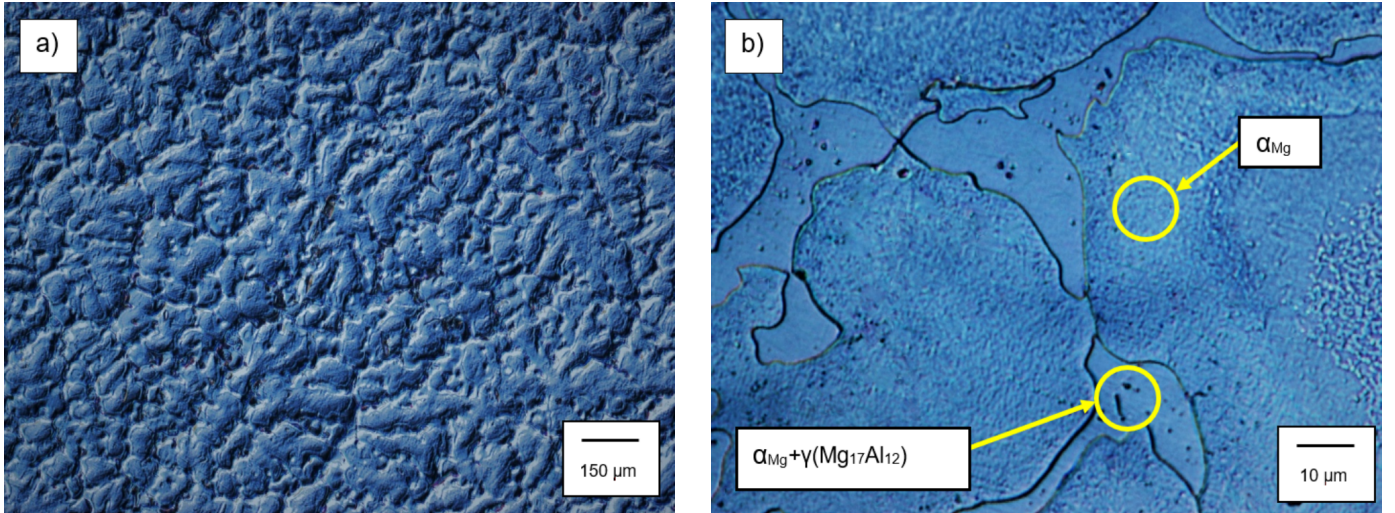


Fig. 3. Microstructure of alloy: a and b – AZ91 + 0.5%Y

oculated with yttrium in the concentration of 0.5%, the biggest microstructure refinement of both phase α_{Mg} and eutectic phase $\alpha_{Mg} + \gamma(Mg_{17}Al_{12})$ was observed. In the images of the microstructures of examined samples, no new phases were observed that could originate from the added yttrium to AZ91 alloy. This is due to the small amount of yttrium, which most probably dissolved in the primary phase α_{Mg} .

According to the Mg-Y equilibrium phase diagram [24], phases $Mg_{24}Y_5$ can be found if the mass concentration of yttrium is above 2%. In this case, yttrium is most likely dissolved in the α_{Mg} phase. In the examined microstructures were not identified phases: αAl_3Y , Al_2Y , probably by too low content of yttrium and aluminum, which also explains the phase equilibrium system Al-Y [25].

However, J. Su et al. in their study [26] demonstrated that, the formation of Al_2Y consumes a part of Al, and the increase in Y content increases the solid solubility of Al, thus reducing the Al of participating eutectic reaction, which leads to a reduction in $\gamma(Mg_{17}Al_{12})$ amount in eutectic phase. The similar conclusion was formulated by L. Liu et. al. in study [27]. Therefore in this study was add only small amount of yttrium, because effect of inoculation is the main part of a wider research program, which will continue by authors.

Image analysis

Fig. 4 shows exemplary microstructure images subjected to a statistical image analysis. The aim of the analysis was to compare the mean change in the grain size of primary phase α_{Mg} and eutectic $\alpha_{Mg} + \gamma(Mg_{17}Al_{12})$ in reference to the non-inoculated alloy AZ91. In order to present the effect of the inoculant addition on the mean sizes of the precipitation of phase α_{Mg} and eutectic $\alpha_{Mg} + \gamma(Mg_{17}Al_{12})$, measurements of the mean perimeter and diameter values for the particular phases were made. The percentage difference of the perimeters P_D of the analyzed phases α_{Mg} and eutectic $\alpha_{Mg} + \gamma(Mg_{17}Al_{12})$ for the inoculated alloys

in reference to the non-inoculated alloy AZ91 was calculated from the formula:

$$P_D = \frac{\overline{P_{in}} - \overline{P_B}}{\overline{P_B}} \cdot 100\% \quad (1)$$

where:

- $\overline{P_D}$ – the calculated difference of perimeters, %
- $\overline{P_{in}}$ – the average perimeter of phases α_{Mg} and $\alpha_{Mg} + \gamma(Mg_{17}Al_{12})$ of the inoculated alloys, μm
- $\overline{P_B}$ – the average perimeter of phases α_{Mg} and $\alpha_{Mg} + \gamma(Mg_{17}Al_{12})$ of AZ91, μm

Additionally, the percentage change in the diameter D_D for the particular phases was calculated from the formula:

$$D_D = \frac{\overline{D_{in}} - \overline{D_B}}{\overline{D_B}} \cdot 100\% \quad (2)$$

where:

- $\overline{D_D}$ – the calculated difference of diameters, %
- $\overline{D_{in}}$ – the average diameter of phases α_{Mg} and $\alpha_{Mg} + \gamma(Mg_{17}Al_{12})$ of the inoculated alloys, μm
- $\overline{D_B}$ – the average diameter of phases α_{Mg} and $\alpha_{Mg} + \gamma(Mg_{17}Al_{12})$ of AZ91, μm

It can be inferred from the diagram that, in the case of the precipitation of primary phase α_{Mg} , for all the examined inoculant concentrations, a lower value of the mean grain perimeter in the alloy in reference to the non-inoculated alloy was obtained. The biggest change was observed for the inoculant concentration of 0.2%, which equalled 12.1%. However, only a slightly smaller change equalling 10.1% was revealed for the yttrium concentration of 0.5%. The smallest change was recorded in the case of the inoculant amount of 0.6% and it equalled about 1%.

In the case of the precipitation of the eutectic phase, it was observed that, with the application of the inoculant in the

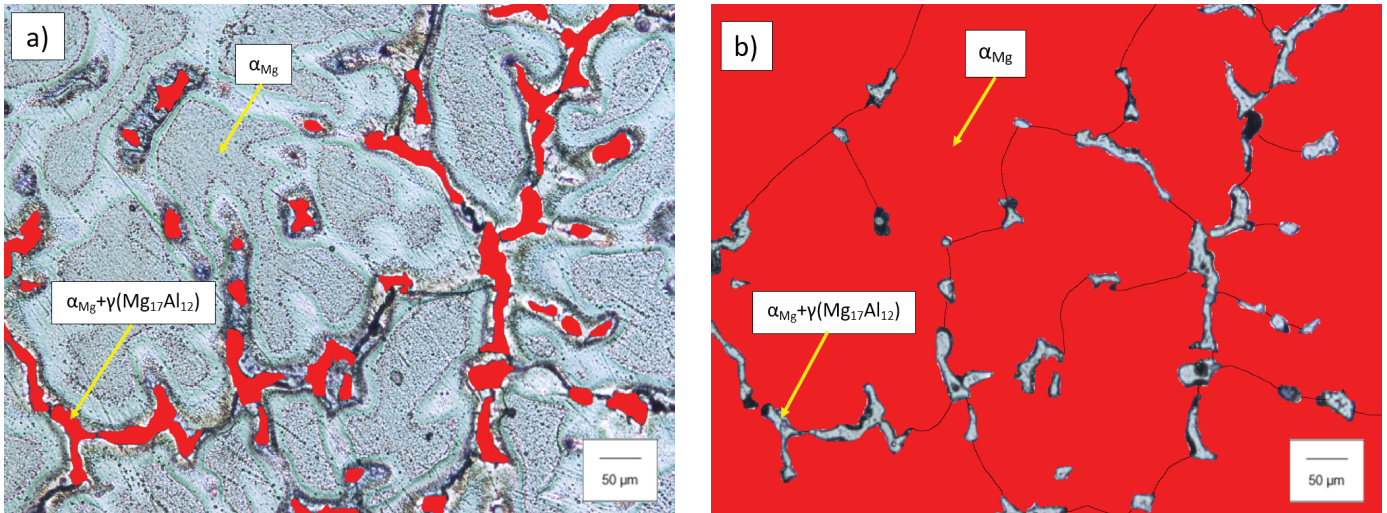


Fig. 4. Microstructure of alloy AZ91 subjected to a statistical image analysis: a – primary phase α_{Mg} and b – eutectic $\alpha_{Mg} + \gamma(Mg_{17}Al_{12})$

concentration of 0.1%, 0.3% and 0.6%, the mean perimeters of the precipitation of phase $\alpha_{Mg} + \gamma(Mg_{17}Al_{12})$ underwent a slight increase in the range from 1.6% to 2.5%. Introducing yttrium in the amount of 0.2% caused an increase of the change in the mean perimeters of the eutectic phase by 18.9%. In turn, within the concentration range from 0.4% to 0.5%, an increase of the value of the mean perimeters of the secondary phase $\alpha_{Mg} + \gamma(Mg_{17}Al_{12})$ was observed, reaching the lowest value for the concentration of 0.5%, which reduced the mean perimeters of the eutectic phase by 5.7%.

Figure 5 shows the value of the index P_D calculated from formula 1.

Figure 6 shows the value of the index D_D calculated from formula 2.

It can be inferred from the presented diagram that an yttrium addition in the amount of 0.2% causes the most intensive changes in the perimeter value in the examined alloys. The grain

perimeters of primary phase α_{Mg} decreased by over 16%, and the grain perimeters of the eutectic increased by nearly 22%. Within the inoculant concentration range from 0.1% to 0.5%, the mean value of the perimeters of primary phase α_{Mg} were reduced. For the inoculant concentration of 0.6%, the value of the mean precipitation perimeter in the alloy stayed practically the same in reference to the non-inoculated alloy.

An yttrium introduction in the amount of 0.1-0.2% as well as 0.6% increases the value of the mean precipitation perimeter of $\alpha_{Mg} + \gamma(Mg_{17}Al_{12})$. For the inoculant concentration equalling 0.3% and 0.4%, the mean perimeters became slightly changed. For the amount of 0.5% of the introduced inoculant, the grain perimeters of the eutectic decreased by 7.1%.

A. Boby et. al. in their research [28] indicate that more than 0.6% of yttrium addition causes decreased of mechanical properties, therefore there was no need to use higher concentration of yttrium in this research.

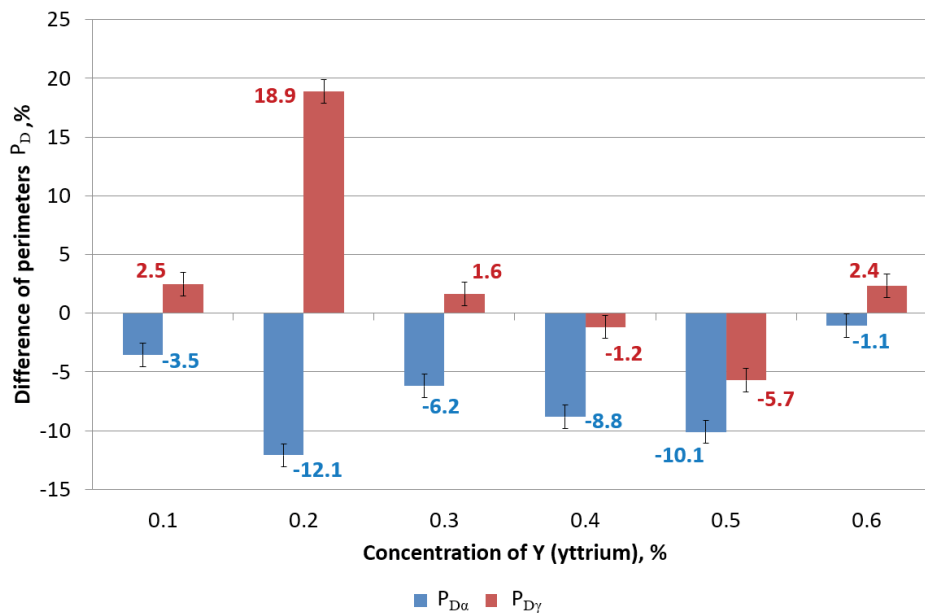


Fig. 5. Change of the grain perimeters of phase α_{Mg} and $\alpha_{Mg} + \gamma(Mg_{17}Al_{12})$ in samples inoculated in reference to AZ91

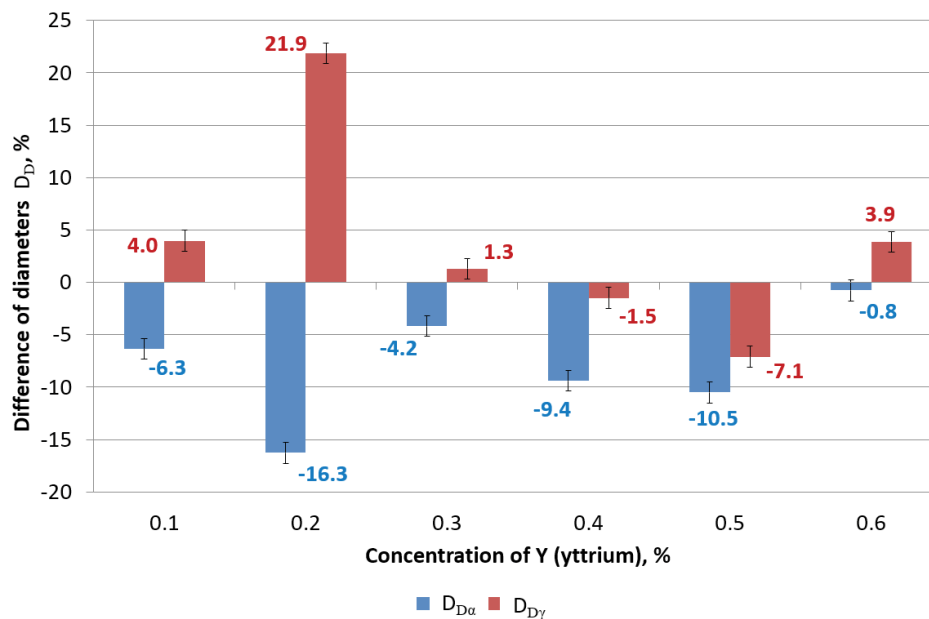


Fig. 6. Change in the mean diameters of phase α_{Mg} and $\alpha_{Mg} + \gamma(Mg_{17}Al_{12})$ in inoculated samples in reference to AZ91

Chemical composition analysis

Using yttrium in that small range has not relevant impact of chemical composition changes. Table 5 compiles the results of the chemical composition analysis for the examined samples, which every alloy is in accordance with the standard PN-EN 1753:2001 [21].

TABLE 5

Chemical composition of analyzed alloys

Chemical composition, % mass					
Melt no.	Mg	Al	Zn	Mn	Si
II	91.8	7.46	0.415	0.255	0.0204
III	91.4	7.94	0.414	0.217	0.0198
IV	91.7	7.65	0.421	0.189	0.0208
V	91.4	7.89	0.430	0.230	0.0197
VI	91.3	7.75	0.648	0.238	0.0215
VII	91.5	7.87	0.429	0.177	0.0147

4. Conclusions

The performed research is an introduction to broader studies aiming to obtain a refinement of the microstructure of casts made of the magnesium alloy AZ91, which, in consequence, should improve the mechanical properties and strength-to-weight ratio of the casts without a significant effect on the chemical composition of the alloy [29]. The analysis of the obtained test results has made it possible to draw the following conclusions:

1. The use of an inoculant in all the examined concentration scopes shortened the crystallization time of phase α_{Mg} , reaching the highest time reduction for the inoculant concentration of 0.2%, whereas for the concentration of 0.6%,

the reduction of the crystallization time of the primary phase was negligibly small. In the case of the eutectic, the shortest solidification time was observed for the alloy in which the inoculant concentration equalled 0.5%.

- The use of yttrium in the amount of 0.1% and in the scope of 0.3% to 0.5% shortens the total crystallization time of the inoculated alloy AZ91 solidifying in a ceramic TDA-sampler. The biggest reduction of the total crystallization time was observed for the concentration of 0.5% and it equalled 23.7 s.
- Introducing yttrium in the concentration of 0.2% causes the most significant changes in the examined alloys, by increasing the perimeters and diameters of the eutectic's grains, at the same time reducing the diameters and the grains of the primary phase.
- The biggest reduction of the perimeters and diameters of the grains of primary phase α_{Mg} and eutectic $\alpha_{Mg} + \gamma(Mg_{17}Al_{12})$ was obtained for the inoculant concentration equaling 0.5%.
- The use of an inoculant in the concentration of 0.6% has practically no effect on the perimeters and diameters of the grain of the primary phase and only slightly changes the perimeters and diameters of the eutectic's grains.
- On the basis of the obtained results, it was assumed that the optimal changes in the microstructure were recorded in the alloy enriched with an inoculant in the concentration of 0.5%.

Acknowledgement

This work was realized within PO WER WSD financed by the National Centre for Research and Development, Poland. Project ID POWR.03.02.00-00-1042/16-00.

REFERENCES

- [1] H. Dieringa et al., Mg Alloys: Challenges and Achievements in Controlling Performance, and Future Application Perspectives, in: Orlov D., Joshi V., Solanki K., Neelameggham N. (Eds.) Magnesium Technology 2018. Cham. The Minerals, Metals & Materials Series (2018).
- [2] T. Rzychoń, Stopy Mg-Al-Ca-Sr przeznaczone do odlewania grawitacyjnego do formpiaskowych. Struktura, właściwości i mechanizmy umocnienia, Wydawnictwo Politechniki Śląskiej (2018).
- [3] C. Dehghanian, M. Lotfipour, M. Emamy, J. Mater. Eng. Perform. (2019), <https://doi.org/10.1007/s11665-019-03978-4>.
- [4] A. Dziadoń, Magnez i jego stopy, Wydawnictwo Politechniki Świętokrzyskiej (2012)
- [5] G. Yuan, G. You, S. Bai, W. Guo, J. Alloy Compd. (2018), <https://doi.org/10.1016/j.jallcom.2018.06.370>.
- [6] B. Mordike, T. Ebert, Mater. Sci. Eng. (2001), [https://doi.org/10.1016/S0921-5093\(00\)01351-4](https://doi.org/10.1016/S0921-5093(00)01351-4).
- [7] C. Rapijko, B. Pisarek, T. Pacyniak, Arch. Metall. Mater. (2017), <https://doi.org/10.1515/amm-2017-0324>.
- [8] W. Liu, B. Jinag, Q. Yang, J. Tao, B. Liu, F. Pan, Prog. Nat. Sci.-Mater. (2019): <https://doi.org/10.1016/j.pnsc.2019.07.002>.
- [9] N. Stanford, R.K.W. Marceau, M.R. Barnett, Acta. Mater. (2014), <http://dx.doi.org/10.1016/j.actamat.2014.09.022>.
- [10] J. Medina, P. Pérez, G. Garcés, P. Adeva, Mater. Charact. (2017), <http://dx.doi.org/10.1016/j.matchar.2017.04.033>.
- [11] X. Wu, M. Chen, R. Qu, Q. Li, S. Guan, T. Jpn. I. Met. (2017), <https://doi.org/10.2320/matertrans.M2016445>.
- [12] A. Afsharnaderi, M. Malekan, M. Emamy, J. R. Ghani, M. Lotfipour, J. Mater. Eng. Perform. (2019), <https://doi.org/10.1007/s11665-019-04396-2>.
- [13] A.V. Kolygin, V.D. Belov, V.E. Bazhenov, (2013), <https://doi.org/10.1134/S0036029513010060>.
- [14] R.C. Bannah, Y. Fu, H. Hao, China Foundry (2019), <https://doi.org/10.1007/s41230-019-9067-9>.
- [15] T.E. Quedsted, A.L. Greer, Acta Materialia. (2005), <https://doi.org/10.1016/j.actamat.2005.06.018>.
- [16] Ch. Jun, Z. Qing, L. Quanan, Amer. Foundry Soc. (2018), <https://doi.org/10.1007/s40962-018-0222-7>.
- [17] W. Huang, X. Yang, Y. Yang, T. Mukai, T. Sakai, J. Alloy Compd. (2018), <https://doi.org/10.1016/j.jallcom.2019.01.269>.
- [18] G. Hu, B. Xing, F. Huang, M. Zhong, D. Zhang, J. Alloy Compd. (2016), <http://dx.doi.org/10.1016/j.jallcom.2016.06.216>.
- [19] Z. Zhao, Q. Chen, F. Kang, D. Shu, J. Alloy Compd. (2009), <https://doi.org/10.1016/j.jallcom.2009.04.059>.
- [20] X. Chen, L. Liu, F. Pan, Mater. Des. (2015), <http://dx.doi.org/10.1016/j.matdes.2014.09.034>.
- [21] PN-EN 1753:2001. Magnesium and magnesium alloys. Magnesium alloy ingots and castings.
- [22] C. Rapijko, B. Pisarek, E. Czekał, T. Pacyniak, Arch. Metall. Mater. (2014), <https://doi.org/10.2478/amm-2014-0246>.
- [23] M. Król, T. Tański, G. Matula, P. Snopiński, A. E. Tomiczek, Arch. Metall. Mater. (2015), <https://doi.org/10.1515/amm-2015-0478>.
- [24] A.R. Mirak, C.J. Davidson, J.A. Taylor, J. Magnes Alloy (2015), <https://doi.org/10.1016/j.jma.2015.06.003>.
- [25] S. Liu, Y. Du, H. Xu, C. He, J. C. Schuster, J. Alloy Compd. (2006), <https://doi.org/10.1016/j.jallcom.2005.06.078>.
- [26] J. Su, F. Guo, H. Cai, L. Liu, J. Phys. Chem. Solids. (2019), <https://doi.org/10.1016/j.jpcs.2019.03.021>.
- [27] L. Liu et al., Materials (2017), <https://doi.org/10.3390/ma10050477>.
- [28] A. Boby, K.K. Ravikumar, U.T.S. Pillai, B.C. Pai, Procedia Engineer. (2013), <https://doi.org/10.1016/j.proeng.2013.03.226>.
- [29] E. Bo, T. Mathia, Patent: Method and apparatus for treating eutectic and eutectoid compositions, United States of America 4, 372 781, 1983.